



저작자표시-비영리-변경금지 2.0 대한민국

이용자는 아래의 조건을 따르는 경우에 한하여 자유롭게

- 이 저작물을 복제, 배포, 전송, 전시, 공연 및 방송할 수 있습니다.

다음과 같은 조건을 따라야 합니다:



저작자표시. 귀하는 원 저작자를 표시하여야 합니다.



비영리. 귀하는 이 저작물을 영리 목적으로 이용할 수 없습니다.



변경금지. 귀하는 이 저작물을 개작, 변형 또는 가공할 수 없습니다.

- 귀하는, 이 저작물의 재이용이나 배포의 경우, 이 저작물에 적용된 이용허락조건을 명확하게 나타내어야 합니다.
- 저작권자로부터 별도의 허가를 받으면 이러한 조건들은 적용되지 않습니다.

저작권법에 따른 이용자의 권리와 책임은 위의 내용에 의하여 영향을 받지 않습니다.

이것은 [이용허락규약\(Legal Code\)](#)을 이해하기 쉽게 요약한 것입니다.

[Disclaimer](#)



공학석사 학위논문

Application of Electrochemical Ion
Separation System for Removing Sodium
Impurity to Produce High Purity KCl

전기화학적 시스템을 적용한 염화칼륨 원료 내
소듐 이온 불순물의 선택적 제거 공정 연구

2018년 2월

서울대학교 대학원

화학생물공학부

윤 한 선

Abstract

Application of Electrochemical Ion Separation System for Removing Sodium Impurity to Produce High Purity KCl

Hansun Yoon

Chemical Convergence for Energy & Environment

School of Chemical and Biological Engineering

Seoul National University

Potassium hydroxide (KOH) is widely used in various industrial fields, especially KOH used in electronic fields has a high economic value because it requires a high purity of 99% or more. At present, KOH is commercially mass-produced by an electrolysis process of potassium chloride (KCl), and thus, the purity of KOH produced is directly influenced by the purity of the raw KCl materials. In the case of industrial raw KCl materials, the impurities are removed by crystallization because they contain sodium ion impurities. However, crystallization has a problem in that a pretreatment process is required when the concentration of the sodium ion impurities is high. In this study, an electrochemical system using sodium manganese oxide

(NMO) and potassium iron hexacyanoferrate (KFeHCF) which can remove sodium ions selectively from the raw KCl material used in the industrial process for KOH production was proposed. As the main results of this study, the NMO/KFeHCF system selectively removed approximately 36% of the sodium ion impurities in the industrial raw KCl solution after 3 cycles of operation. The purity of KCl was increased to 99.8% or more; thus, it was possible to produce high purity KOH with high economic value.

Keyword: Electrochemical system, Impurity removal, Ion separation, Sodium, Potassium

Student number: 2016-20995

Contents

List of Figures	V
Chapter 1. Introduction	1
Chapter 2. Literature Review	4
2.1 Potassium hydroxide (KOH) production	4
2.1.1 Use of KOH	4
2.1.2 Electrolysis of potassium chloride (KCl).....	5
2.2 Electrochemical sodium ion separation technology.....	8
2.2.1 Desalination	9
2.2.2 Impurity removal	13
2.3 Electrode materials.....	14
2.3.1 Sodium manganese oxide ($\text{Na}_{0.44}\text{MnO}_2$).....	14
2.3.2 Prussian blue and its analogues	18

Chapter 3. Materials and Method	21
3.1 Material synthesis and electrode fabrication.....	21
3.1.1 Sodium manganese oxide (NMO) electrode	21
3.1.2 Potassium iron hexacyanoferrate (KFeHCF) electrode	23
3.2 Electrochemical characteristics analysis.....	26
3.2.1 Cyclic voltammetry	26
3.2.2 Galvanostatic charging/discharging	26
3.3 Sodium removal performance test	27
Chapter 4. Results & Discussion.....	30
4.1 Electrochemical characteristics of electrodes	30
4.2 Sodium removal with NMO/KFeHCF system.....	34
4.3 Industrial application of NMO/KFeHCF system	37
Chapter 5. Conclusion	40
References	41
국문초록	45

List of Figures

Figure 1. The membrane cell electrolysis process of potassium chloride.....	7
Figure 2. (a) Schematic diagram of operations steps of the desalination battery.	
(b) Cell voltage versus applied charge in the desalination battery. (Pasta et al., 2012b).....	11
Figure 3. Schematic diagram of operations steps of the rocking chair desalination battery. (Lee et al., 2017).....	12
Figure 4. The concentration changes (a) after the ion capturing process in the solution containing 30 mM of NaCl, KCl, MgCl ₂ , and CaCl ₂ . (b) after ion releasing process in 30 mM LiCl. (Kim et al., 2017).....	16
Figure 5. Cyclic voltammograms of Na _{0.44} MnO ₂ electrode in 1 M NaCl, KCl, MgCl ₂ , and CaCl ₂ . (Kim et al., 2017)	17
Figure 6. The structure of Prussian blue analogue (PBA), nickel hexacyanoferrate (Wang et al., 2013).....	20
Figure 7. (a) XRD patterns of the NMO used in this study and peak position of NMO in reference (JCPDS 27-0750) (b) SEM image (before ball-milled) of the NMO used in this study.....	22
Figure 8. (a) XRD patterns and (b) SEM image of the KFeHCF used in this study.	25
Figure 9. Schematic of the NMO/KFeHCF system operation for sodium ion removal and electrode regeneration	29

Figure 10. The cyclic voltammograms of (a) NMO electrode (NaCl, 1 M; black solid line & KCl, 1 M; blue dotted line) and (b) KFeHCF electrode (KCl, 1 M) (scan rate: 1 mV/s)32

Figure 11. Galvanostatic charging and discharging voltage profile of (a) NMO electrode (NaCl 1 M; current density: 0.01 A/g) and (b) KFeHCF electrode (KCl 1 M; current density: 0.1 A/g)33

Figure 12. The concentration ratio of the sodium and potassium ions after (a) the sodium ion removal step (1st step) in the target KCl solution ($C_{0, K^+} = 40$ mM; $C_{0, Na^+} = 20$ mM) (current density: 0.3 mA/cm², 1 h) and (b) the electrode regeneration step (3rd step) in the reservoir KCl solution (C_{0, K^+} or $N_{a^+} = 20$ mM, actual sodium ions are not present in the reservoir solution, but the C_0 of Na^+ was set to 20 mM to represent the concentration ratio)36

Figure 14. (a) The concentration ratio of sodium ions and (b) the voltage profile of the 1st step (sodium ion removal step) & 3rd step (electrode regeneration step) for 3 continuous cycles of operation in the industrial KCl solution (~ 4 M KCl solution with 20 mM NaCl as the impurity)39

Chapter 1. Introduction

Potassium hydroxide (KOH) is widely used as a chemical reagent required in various industrial fields such as semiconductor processing and the manufacturing of potassium compounds, pharmaceuticals and synthetic resins. In particular, the economic value of KOH used for surface etching in the field of semiconductor processing has increased because the KOH used in this field requires a high purity of 99.8% or more. At present, KOH is commercially mass-produced through electrolysis of a potassium chloride (KCl) solution; thus, the purity of KOH is directly affected by the purity of the raw KCl materials. Because the raw KCl materials used for industrial purposes contain NaCl salts as the main impurities, it requires an additional process for the purity control of KOH such as a crystallization method. However, the crystallization method cannot function effectively in a KOH solution which contains sodium ion impurities of 200 mg/kg or more (Osakabe et al., 2009). Thus, a pretreatment process to remove the sodium ion impurities for highly purified KOH production is necessary.

Electrochemical systems using battery materials can be proposed as an alternative or the pretreatment process for the crystallization method. Recently, selective ion separation systems using battery materials have been actively studied as a next generation technology. A desalination battery system based on a mixing entropy battery system using salinity difference has emerged as an environmentally friendly and energy efficient desalination technology (La Mantia et al., 2011; Pasta

et al., 2012b). The technology utilizing such electrochemical battery systems has been applied not only to desalination but also to resource recovery. As a representative example, a technique for selectively extracting and recovering lithium ions from the brine has been studied (Kim et al., 2015; Lee et al., 2013; Pasta et al., 2012a). Additionally, HCDI (hybrid capacitive deionization) systems have been studied with great potential as a desalination technology for brackish water because of its simple process and high energy efficiency (Kim et al., 2016; Lee et al., 2014b). In a HCDI system, cation selective battery materials are applied with a counter carbon electrode which can lead to better deionization performance compared to the conventional CDI system (Anderson et al., 2010). Although these electrochemical systems with battery materials are expanding their applications based on their selective ion separation function, there are few studies on the purity control or on the selective removal of ion impurities. A selective ion separation system can be applied to the impurity removal process in a situation where specific ions become impurities. If sodium ion impurities are to be selectively removed, sodium ion battery materials which are known to selectively intercalate sodium ions can be used (Kim et al., 2017; Sauvage et al., 2007b).

When removing sodium ion impurity in the presence of potassium ions, Prussian blue analogues (PBA), which have an open framework structure capable of capturing cations such as Na^+ and K^+ , can be used as a counter electrode (Lee et al., 2014a; Lu et al., 2012; Wessells et al., 2011). Prussian blue is commonly used as a pigment or medicine to adsorb cesium; however, the application of PBA has been

extended to aqueous battery materials because of their low cost and stability in an aqueous system (Karyakin, 2001; Pasta et al., 2012c; Su et al., 2017; Trócoli et al., 2015). In this study, the principle of a rocking chair battery system (Scrosati, 1992) was applied to a selective sodium ion removal process to improve the purity of a KCl solution. It is expected that the electrochemical system consisted of a sodium manganese oxide (NMO) electrode for capturing sodium ions and a potassium iron hexacyanoferrate (KFeHCF, a kind of PBA) electrode for capturing potassium ions can selectively remove sodium ions.

This study demonstrated that an electrochemical system can be applied as an impurity removal technique in the manufacturing industry for potassium products as a simple, energy efficient and low cost method. Thus, this study investigated how the NMO/KFeHCF system works with a specific ion exchange behavior. The applicability to an actual industry was also tested using a raw material (~ 4 M KCl) that is used in the industrial process for KOH production.

Chapter 2. Literature Review

2.1 Potassium hydroxide (KOH) production

2.1.1 Use of KOH

Potassium hydroxide (KOH), also called caustic potash, is an inorganic chemical reagent widely used for various kinds of applications. It is useful in many industrial fields including the production of potassium containing chemicals, manufacture of soft and liquid soaps, fertilizer production, fabrication of alkaline batteries and semiconductor processing.

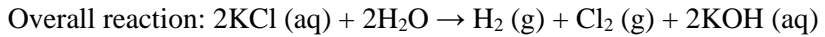
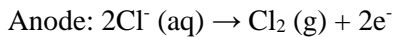
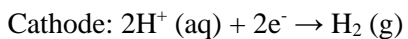
KOH reacts well with chemical species such as acids through a neutralization reaction because of the alkaline characteristic of it. Such acid-base reaction is used for the production of the potassium containing chemicals like carbonate or phosphate salts of potassium and these produced potassium salts are also used for many applications. (Schultz et al., 2000) The reaction of fats and oil with KOH, called saponification, is applied to the production of potassium soaps. The potassium soap has a highly water-soluble characteristic compared to the soaps produced with sodium hydroxide, so it is usually used for the soft or liquid soap manufacturing. KOH is also a raw material of the agriculture grade fertilizer industry. The fertilizer containing KOH acts as a potassium source for crops because potassium is one of the major contents of plant nutrition.

KOH has recently expanded its application to batteries and electronic materials. An aqueous solution of KOH is employed as the electrolyte in some types

of alkaline batteries like nickel-cadmium, nickel-hydrogen and nickel metal hydride battery. In the industrial fields of semiconductor processing, KOH is used as a silicon etchant removing monocrystalline on a silicon wafer. When used in electronics fields such as surface etching, the purity of KOH affects the quality of product. Thus, the economic value of high purity KOH has increased because the KOH used in these fields requires a high purity of 99.8% or more.

2.1.2 Electrolysis of potassium chloride (KCl)

Today, KOH is commercially mass-produced through the electrolysis of potassium chloride (KCl) solution. KCl electrolysis is very similar to the electrolysis of sodium chloride, which is well known as a chlor-alkali process. Potassium hydroxide and chlorine gas are produced by the electrolysis of aqueous chloride solution according to following reactions:



At the cathode, hydroxide ions and hydrogen gas are produced together with water decomposition reaction when chloride ions are oxidized to chlorine gas at the anode. Due to the importance of separating these electrolysis products, some cell designs such as diaphragm cells, mercury cells, and membrane cells were devised.

The diaphragm cell is composed with a porous solid separator (ex. asbestos)

between the two electrode compartments. When the solution containing chloride salts is fed to the anode compartment, hydroxide chemical is produced in the separated cathode compartment. In the mercury cell, hydrogen gas and potassium hydroxide are produced at the mercury cathode through making the amalgam as an intermediate product. Although this method has the advantage of obtaining higher purity KOH than when using diaphragm cells, it has some economic and environmental problems.

In recent years, the membrane cell with enhanced electrolytic efficiency has emerged using a membrane as a separator. (Bergner, 1982) The membrane between the two electrodes only allows the cations permeation, so the potassium ion supplied to the anode side can combine with the hydroxide ion at the cathode side to produce KOH. This method gives about 30% concentration of KOH solution and further crystallization and distillation processes can increase the purity of the product. The purity of the produced KOH is also directly influenced by the purity of the KCl raw material, thus it is also important to control the purity of KCl.

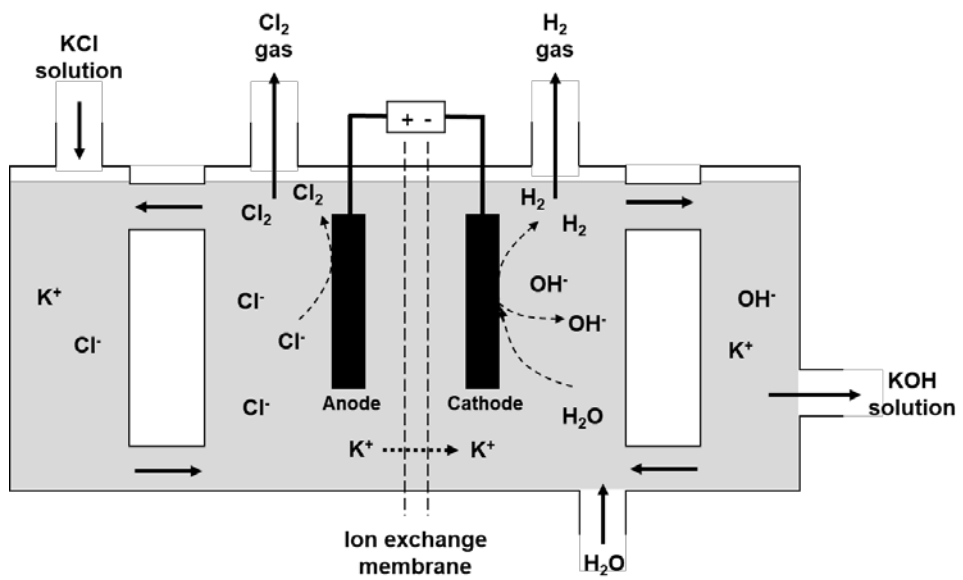


Figure 1. The membrane cell electrolysis process of potassium chloride.

2.2 Electrochemical sodium ion separation technology

Typical technologies previously used for ion separation include distillation, membrane filtration, and ion exchange process. However, these processes have disadvantages like complexity of the process operation, high energy consumption, and high operation cost and time. Electrochemical ion separation process, which is a combination of electrochemical energy and electrode material research, has been actively studied to overcome the drawbacks of the existing technologies, and it is attracting a great attention as a next generation technology. The complex separation process is simplified by applying battery and capacitive ion storage systems, and it is developed as a highly efficient technology in terms of energy, time, and cost. The application of electrochemical ion separation process has been expanded variously. In particular, the sodium ion selective materials were applied to achieve specific purposes such as desalination and impurity removal.

2.2.1 Desalination

Capacitive deionization (CDI) is a well-known technology for the electrochemical ion separation processes in the field of water desalination. CDI separates and removes charged substances from aqueous solutions based on the principle of electrosorption. By applying a voltage to a CDI cell composed of a pair of electrodes, ionic species are captured to each electrode. The electrodes are typically fabricated with porous carbon, so the ions migrate non-selectively into electrical double layers formatted around a pore surface. (Farmer et al., 1995) Recently, a hybrid CDI (HCDI) system with a faradaic electrode instead of a carbon electrode on one side was studied. Selective ion removal was possible due to the sodium ion selective characteristic of faradaic electrodes(sodium manganese oxide (Lee et al., 2014b) and sodium iron pyrophosphate (Kim et al., 2016)) and salt adsorption capacity was also increased to over 30 (mg NaCl)/(g of electrode).

The electrochemical ion separation process using battery electrodes and system also developed with the expansion of CDI research. Desalination battery is the first application to water desalination. (Pasta et al., 2012b) The desalination battery reversed the stage of the mixing entropy battery system, which produces electrical energy using the salinity difference between seawater and river. (La Mantia et al., 2011) The battery system composed of $\text{Na}_2\text{Mn}_5\text{O}_{10}$ and Ag/AgCl electrodes removed Na^+ and Cl^- ions in seawater by consuming electrical energy with four steps of figure 2(a). At the step 1, a constant current is applied to the electrochemical cell and ions are removed from the solution. After replacing seawater solution to fresh

water solution at step 2, the captured ions are released from the electrodes at step 3. Finally, the concentrated solution is changed to new seawater solution (step 4) and this system can be operated with continuous cycles. As a result of one cycle operation, 0.29 Wh/L of energy consumption, comparable to the reverse osmosis (RO) process (0.2 Wh/L), was required to remove 25% of salts.

Lee et al. studied a rocking chair desalination battery system using two kinds of Prussian blue derivative electrodes. (Lee et al., 2017) The system is designed to allow ions to move through the rocking chair principle traditionally used in lithium ion batteries. Conventional electrochemical desalination systems were capable of desalination only during one of the charging or discharging processes. The new cell design (Figure 3) overcomes these drawbacks, enabling desalination in both charging and discharging steps, and maximizing desalination capacity (59.9 mg/g) through efficient operation.

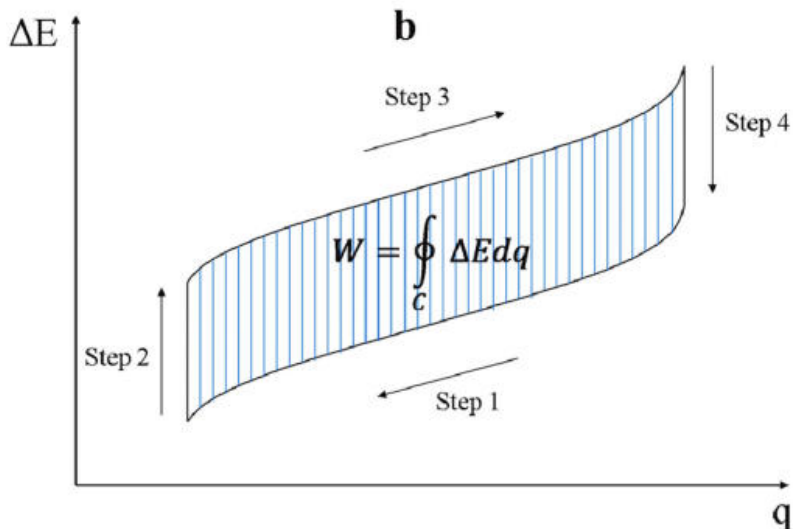
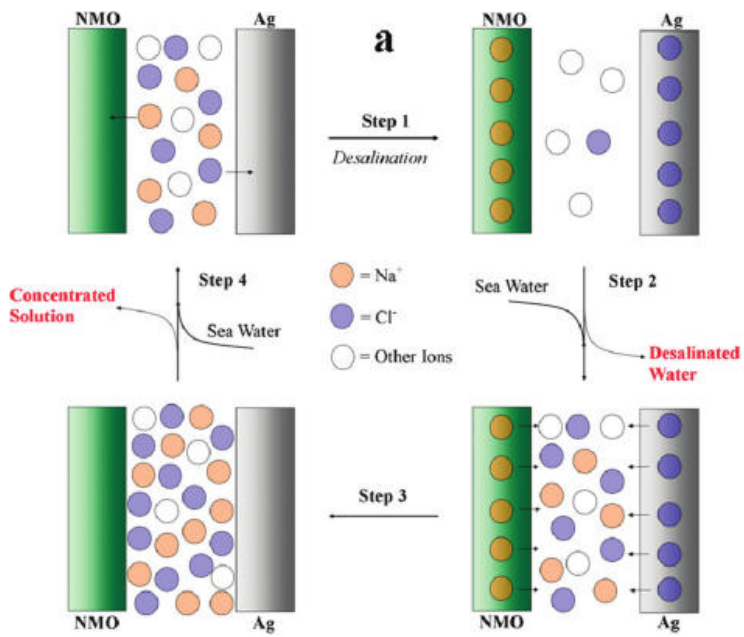


Figure 2. (a) Schematic diagram of operations steps of the desalination battery. (b) Cell voltage versus applied charge in the desalination battery. (Pasta et al., 2012b)

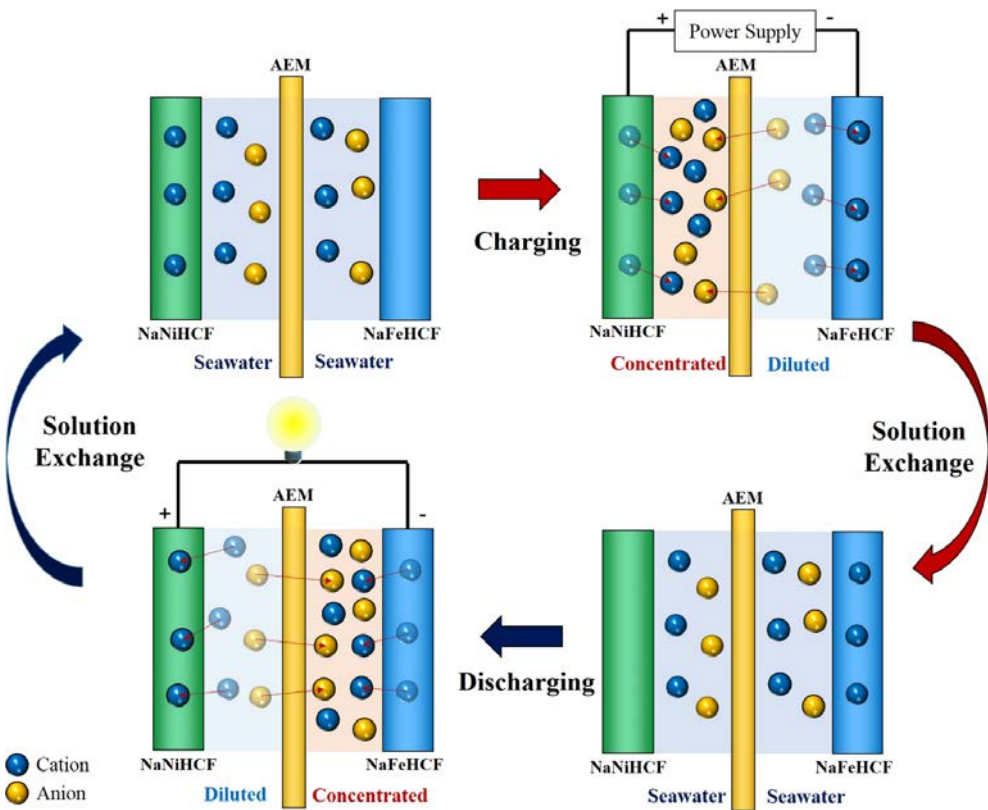


Figure 3. Schematic diagram of operations steps of the rocking chair desalination battery. (Lee et al., 2017)

2.2.2 Impurity removal

Processes for obtaining high purity chemicals have been studied importantly in research and industry. When a chemical raw material containing high impurity contents is used, a problem such as a side reaction due to impurities may occur in the process of production. The electrochemical ion separation process has a possibility to be applied for the impurity control process in that it can selectively separate small amounts of impurities in an energy efficient and environmentally friendly method. The NMO/Ag electrode system of the desalination battery, which was proposed for the purpose of desalination, was successfully applied for separating a small amount of NaCl impurities contained in the KCl raw material for industrial purposes. (Kim et al., 2017) However, due to the economic problem of silver electrode, it is difficult to be applied for a real industry.

2.3 Electrode materials

2.3.1 Sodium manganese oxide ($\text{Na}_{0.44}\text{MnO}_2$)

Na_xMnO_2 materials satisfying $\text{Na}/\text{Mn} \leq 1$ were first reported in 1971, and $\text{Na}_{0.44}\text{MnO}_2$ (NMO) with an orthorhombic structure was also studied. (Parant et al., 1971) Doeuff et al. noted that 3-dimensional manganese oxides have large tunnels to insert ions, so the orthorhombic NMO was applied as the cathode of an alkali metal secondary battery. NMO was found to reversibly intercalate sodium and lithium ions, and its reversibility and stability were demonstrated in a lithium cell. (Doeuff et al., 1994) Sauvage et al. obtained pure NMO without Mn_2O_3 -bixbyte impurity by controlling the conditions of solid state synthesis, and studied the insertion/deinsertion mechanism of sodium ion in NMO structure. The behavior of sodium ion insertion in Na_xMnO_2 was analyzed to be reversible in the range of $0.25 < x < 0.65$ and irreversible at $x < 0.25$ range. (Sauvage et al., 2007b) The application for a positive electrode of energy storage device was evaluated in an aqueous electrolyte (1 M Na_2SO_4). The rate capability and cyclic durability of NMO were documented with promising performance in NMO/activated carbon electrode system. (Whitacre et al., 2010)

The sodium ion selectivity of NMO was analyzed based on the potentiometric response in aqueous condition. The possibility of NMO for the sodium ion sensor was demonstrated with the results of Nernstian-like response for Na^+ and good selectivity towards Li^+ , K^+ , Mg^{2+} , and Ca^{2+} . (Sauvage et al., 2007a)

This selectivity of NMO was also demonstrated by ion capturing experiments of an electrochemical system consisting of NMO and Ag/AgCl. After the ion capturing process in the solution containing equal concentrations of respective Na^+ , K^+ , Mg^{2+} , and Ca^{2+} ions, the electrochemical selectivity was evaluated by analyzing the change in concentration of each ion. The results in Figure 4 showed that the selectivity of NMO for Na^+ was obtained 13 times higher than for K^+ and 6 - 8 times higher than for Mg^{2+} , and Ca^{2+} . The electrochemical reactivity data in Figure 5 from cyclovoltammetric analysis also supported this result by showing clear peaks for only sodium ion. (Kim et al., 2017)

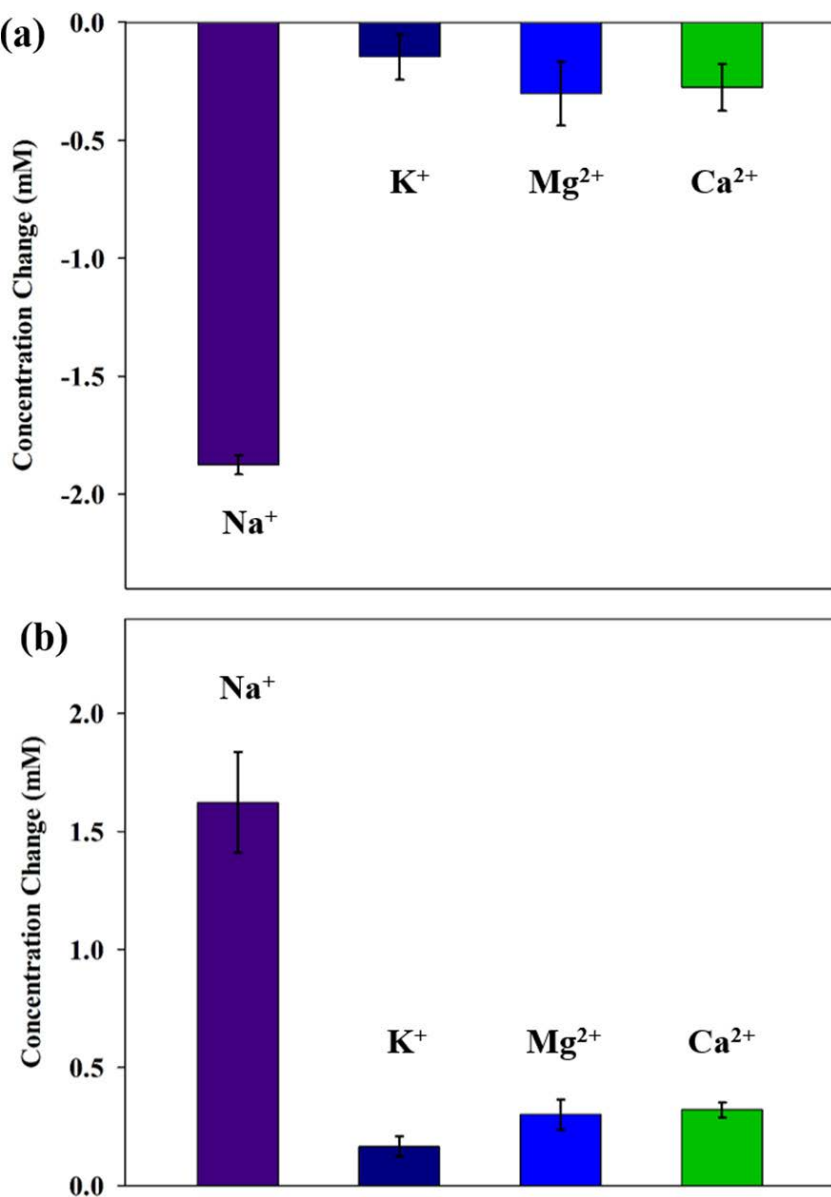


Figure 4. The concentration changes (a) after the ion capturing process in the solution containing 30 mM of NaCl , KCl , MgCl_2 , and CaCl_2 . (b) after ion releasing process in 30 mM LiCl . (Kim et al., 2017)

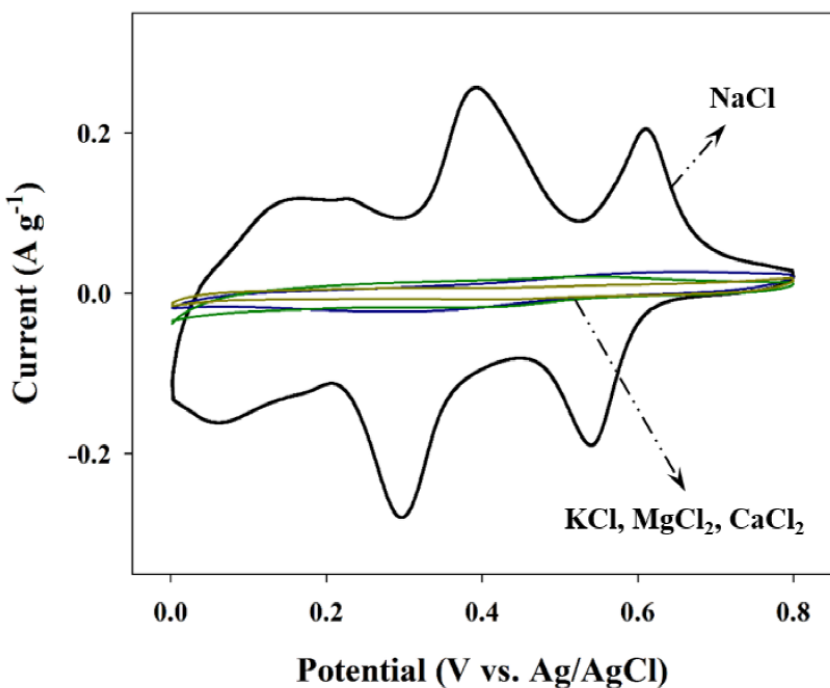


Figure 5. Cyclic voltammograms of $\text{Na}_{0.44}\text{MnO}_2$ electrode in 1 M NaCl , KCl , MgCl_2 , and CaCl_2 . (Kim et al., 2017)

2.3.2 Prussian blue and its analogues

Prussian blue, or ferric hexacyanoferrate is a coordination material that has been used as a synthetic pigment for a long time. Recently, the application field was expanded as an energy storage material due to the open framework structure of Prussian blue. Prussian blue having a formula of $\text{Fe}_4[\text{Fe}(\text{CN})_6]_3$ has a face-centered cubic structure that iron atoms with divalent and trivalent oxidation states are connected to $\text{C}\equiv\text{N}$ ligand pairs. When Fe^{2+} and Fe^{3+} are replaced by different kinds of transition metal elements, they are called Prussian blue analogues (PBA). PBA is represented by general formula of $\text{A}_x\text{M}_{(1)}[\text{M}_{(2)}(\text{CN})_6]_y$ where $(\text{M}_{(1)}, \text{M}_{(2)}) = \text{Fe}, \text{Mn}, \text{Co}, \text{Ni}, \text{Cu}, \text{Zn}$, and $\text{A} = \text{Li}, \text{Na}, \text{K}, \text{Rb}$. (Paoletta et al., 2017) Various types of PBA can be formed depending on the constituent elements, all of which have 3-dimensional diffusion channels that can intercalate alkali ions in the structure. As shown in Figure 6, cations such as Na^+ and K^+ can be occupied in A sites in the middle of the eight subcells of a unit cell. (Wessells et al., 2011)

PBA has been studied as an aqueous sodium and potassium battery material based on the structure capable of intercalating alkaline ions and on the stability in aqueous systems. Wessells et al. used nickel hexacyanoferrate, a kind of PBA, as an electrode material, and carried out the insertion/extraction of sodium and potassium ions over 5,000 cycles without critical loss of capacity. It has been proven that PBA can be easily synthesized at low cost, and has good durability, safe and energy-efficient characteristics. Therefore, it has attracted attention as a material that can be used for divalent as well as monovalent ion batteries. (Wang et al., 2015; Wu et al.,

2013; Wu et al., 2015) Additionally, Trocoli et al. solved the high cost problem of the electrochemical lithium recovery system by replacing Ag/AgCl, which was used as a counter electrode, with nickel hexacyanoferrate. (Trócoli et al., 2015; Trócoli et al., 2016)

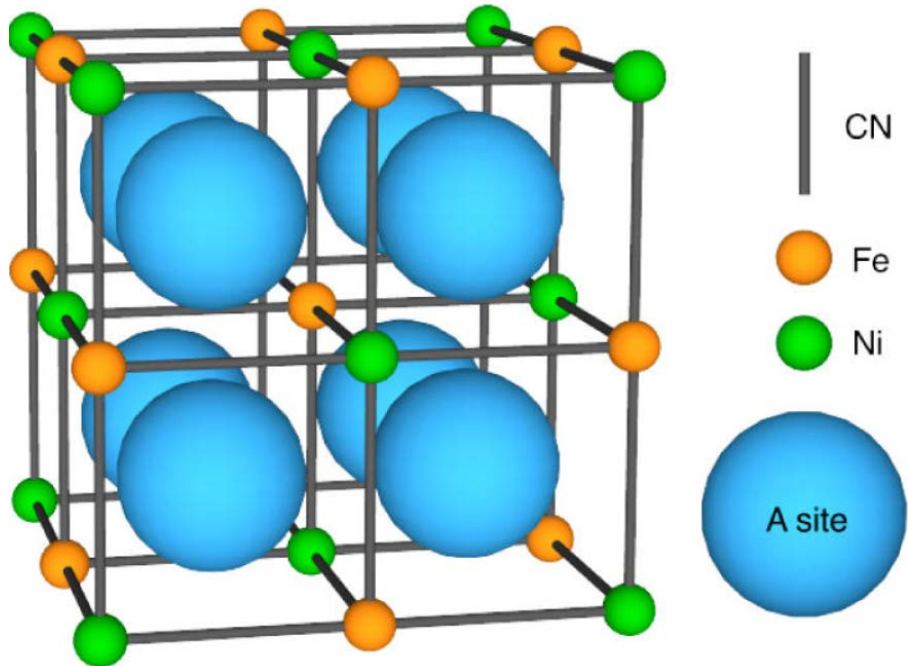


Figure 6. The structure of Prussian blue analogue (PBA), nickel hexacyanoferrate (Wang et al., 2013)

Chapter 3. Materials and Method

3.1 Material synthesis and electrode fabrication

3.1.1 Sodium manganese oxide (NMO) electrode

The sodium manganese oxide ($\text{Na}_{0.44}\text{MnO}_2$, NMO) powder used in this study was synthesized by a solid-state reaction (Lee et al., 2014b). Na_2CO_3 (Sigma-Aldrich) and MnCO_3 (Sigma-Aldrich) were mixed well at a 0.242:1 molar ratio. The precursor of the solid reaction was heated in an electric furnace (MF-12GH, JEIO Tech) at 500 °C for 5 h under atmospheric condition. The mixing process was repeated one more time and then heated at 900 °C for 12 h under atmospheric condition. The obtained material was ball-milled and filtered to obtain the NMO powder.

The NMO powder was analyzed by X-ray powder diffraction (XRD, D8 Discover) and scanning electron microscopy (SEM, FESEM, JEOL JSM 6700 F). Figure 7 shows the structural characterization of the NMO particles used in this study. The XRD pattern of the NMO matched well with the reference (JCPDS 27-0750) and the SEM image shows a rod-type shape of the NMO particles.

The NMO electrode was prepared with the following procedures. $\text{Na}_{0.44}\text{MnO}_2$ active material, carbon black (Timcal) and a binder (polytetrafluoroethylene, PTFE, Sigma-Aldrich) were mixed at a mass ratio of 86:7:7. The sample was placed in a roll-presser to produce a sheet-type electrode with a 250 μm thickness. The electrode was placed in a vacuum oven and dried at 80 °C for 12 h to evaporate the remaining solvent.

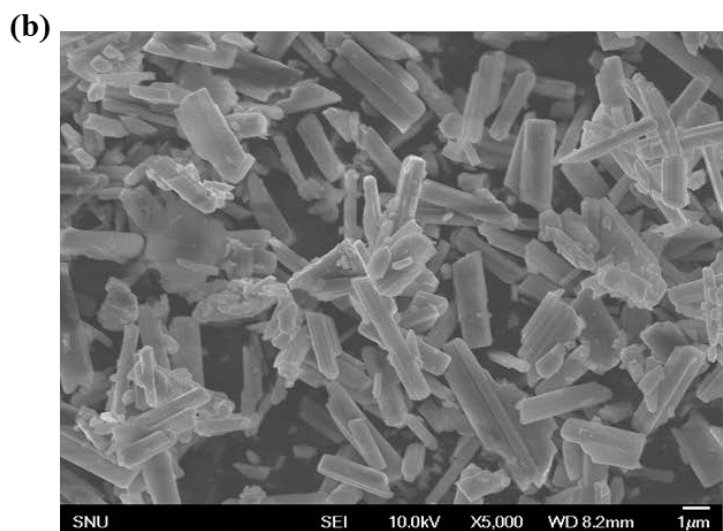
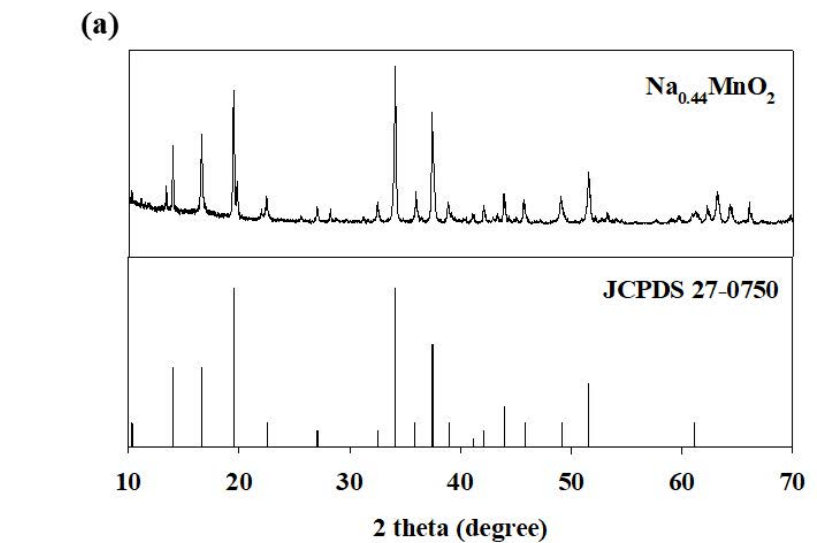


Figure 7. (a) XRD patterns of the NMO used in this study and peak position of NMO in reference (JCPDS 27-0750) (b) SEM image (before ball-milled) of the NMO used in this study

3.1.2 Potassium iron hexacyanoferrate (KFeHCF) electrode

Potassium iron hexacyanoferrate ($K_xFe[Fe(CN)_6]$, KFeHCF) powder used in this study was synthesized by a controlled crystallization reaction. 100 ml of a mixed solution of $FeCl_2 \cdot 4H_2O$ (0.05 M, Sigma-Aldrich) and potassium citrate (0.4 M, Sigma-Aldrich) and 100 ml of potassium hexacyanoferrate (II) (0.05 M, Sigma-Aldrich) were slowly dropped at the same time and stirred for 24 h. The temperature was kept at 25 °C, and KFeHCF powder was obtained by filtering the submerged blue material.

The composition of synthesized powder was analyzed by inductively coupled plasma atomic emission spectrometer (ICP-AES, VARIAN 730ES). The K/Fe molar ratio of KFeHCF was analyzed to be 1.73/1, indicating that the synthesized material has a ‘Potassium-rich’ form. The physical characterization of the KFeHCF powder was analyzed by XRD and SEM methods. Figure 8 shows the structural characterization of KFeHCF particles used in this study. The XRD patterns of the KFeHCF matched well with those of potassium iron hexacyanoferrate nanocubes synthesized from aqueous solution obtained by Su et al. (Su et al., 2017) The SEM image shows that the KFeHCF has a cubic framework which is common structural characteristics of Prussian blue analogues.

The KFeHCF electrode was also fabricated with the following procedures. KFeHCF active material, carbon black (Timcal) and a PTFE binder were mixed at a

mass ratio of 7:1:2. The sheet-type electrode was manufactured with the same method of NMO electrode manufacturing.

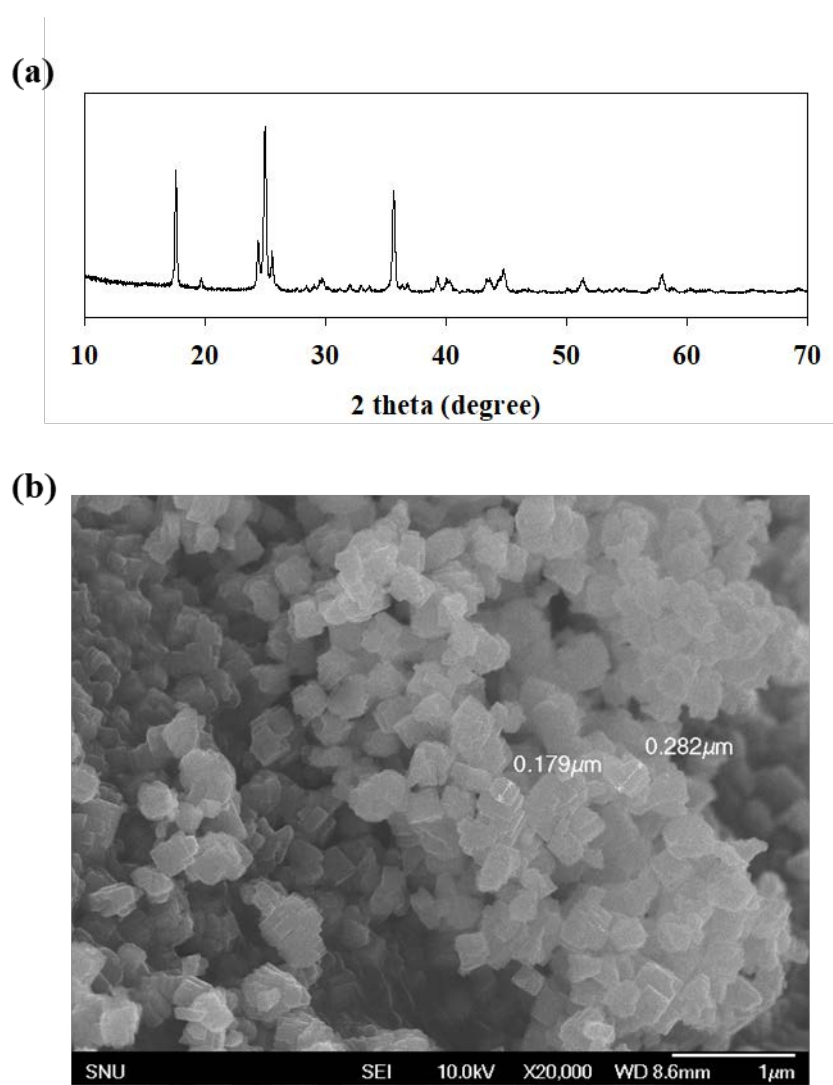


Figure 8. (a) XRD patterns and (b) SEM image of the KFeHCF used in this study.

3.2 Electrochemical characteristics analysis

3.2.1 Cyclic voltammetry

The Cyclic voltammetry (CV) was measured by a potentiostat/galvanostat device (PARSTAT 2273, Princeton Applied Research) using a three electrode cell with a working electrode (NMO or KFeHCF), counter electrode (Ag/AgCl) and a reference electrode (Ag/AgCl electrode, sat'd KCl). A glass microfiber filter (Whatman) was used as a separator and the scan rate was 1 mV/s in a 1 M NaCl and 1 M KCl solution.

3.2.2 Galvanostatic charging/discharging

The galvanostatic charging/discharging was done with a battery cycler (WBCS3000, WonA Tech Co.) using a three electrode cell with a working electrode (NMO or KFeHCF), counter electrode (Ag/AgCl) and a reference electrode (Ag/AgCl electrode, sat'd KCl). A glass microfiber filter (Whatman) was used as a separator and the current density was 0.01 A/g in a 1 M NaCl or KCl solution (in case of NMO electrode) and 0.1 A/g in a 1 M KCl solution (in the case of KFeHCF electrode)

3.3 Sodium removal performance test

The NMO and KFeHCF electrodes were cut into a $2.5 \times 3.5 \text{ cm}^2$ shape and attached to a titanium plate as a current collector with a carbon adhesive. The NMO electrode was charged to 0.9 V (vs. Ag/AgCl, sat'd KCl) to remove the sodium ions in the electrode. Figure 9 schematically shows the NMO/KFeHCF system used in this study. The operation process of the system consists of four steps. The main steps are the sodium ion removal step (1st step) and electrode regeneration step (3rd step). The 2nd and 4th steps are the process of replacing the solution. The system was operated in a three electrode mode using NMO as a working electrode, KFeHCF as a counter electrode and Ag/AgCl (sat'd KCl) as a reference electrode.

During the sodium ion removal step (1st step), sodium ions in the target KCl solution were removed in a current condition of 2.625 mA (0.3 mA/cm^2) by connecting the NMO electrode without sodium ions and the KFeHCF electrode containing potassium ions. As a target KCl solution, 20 ml of a mixed solution (20 mM NaCl and 40 mM KCl) and the industrial KCl solution (~ 4 M KCl) containing 20 mM NaCl as impurities were used. The industrial KCl solution is an actual raw material used in the KOH production process (provided by UNID company, Republic of Korea) and NaCl is the largest impurity component of it. In the 2nd step, the target solution was replaced with the reservoir solution (20 mM KCl solution). In the electrode regeneration step (3rd step), a current of 2.625 mA (0.3 mA/cm^2) was applied in the opposite direction to that of 1st step, so that the sodium ions inserted

into the NMO electrode were released, and the potassium ions were inserted into the KFeHCF electrode. Steps 1 to 4 represent 1 cycle, and several cycles can be operated continuously to remove sodium ions repeatedly. For the system operation, a battery cycler (WBCS3000, WonATech Co.) was used and the cation concentration was measured by ion chromatography (IC, DX-120, DIONEX).

The coulombic efficiency is calculated according to the following equation;

$$\eta_c(\%) = \frac{z_i F \Delta n}{\Sigma} \times 100$$

, where z_i is the ion valance; F is the Faraday constant; Δn is the molar change amount of the ion, and Σ is the total charge transferred at the operating steps, respectively.

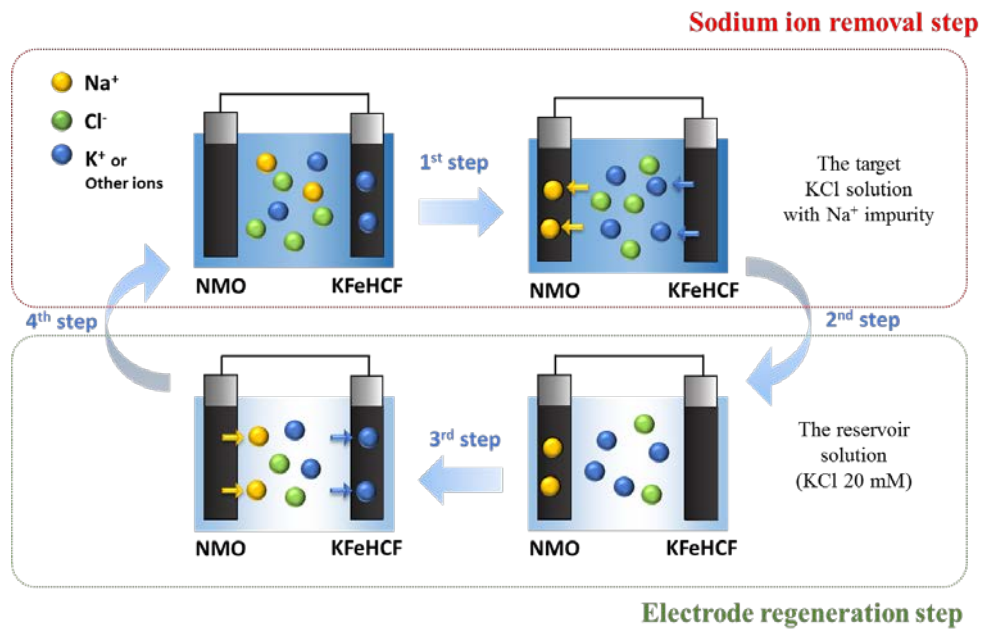


Figure 9. Schematic of the NMO/KFeHCF system operation for sodium ion removal and electrode regeneration

Chapter 4. Results & Discussion

4.1 Electrochemical characteristics of electrodes

Figure 10 shows the CV data of the NMO electrode in 1 M NaCl (black, solid) and 1 M KCl (blue, dotted) and KFeHCF electrode in 1 M KCl to analyze reversible intercalation and deintercalation of the sodium ions with the NMO electrode and those of the potassium ions with the KFeHCF electrode.

As shown in Figure 10(a), four or more oxidation and reduction peaks are paired with each other between 0 V and 0.8 V (vs. Ag/AgCl, sat'd KCl). The sodium ion intercalation peaks were apparent at 0.53 and 0.29 V and showed more than two peaks in the 0 - 0.2 V range. The sodium ion deintercalation peaks were apparent at 0.66 and 0.43 V and showed more than two peaks in the 0.1 - 0.3 V range. According to galvanostatic charging/discharging (refer to Figure 11(a)), more than four flat voltages also appeared in the 0 - 0.6 V range. This is consistent with the CV data and the results of previous studies (Kim et al., 2013; Whitacre et al., 2010). On the other hand, there was no distinct peak in KCl. It shows that the NMO electrode has a selectivity for sodium ions over potassium ions. The good selectivity of the NMO over potassium ions was also demonstrated by the potentiometric method (Sauvage et al., 2007a; Tani and Umezawa, 1998) and by the ion capturing experiment (Kim et al., 2017), and these results enable selective sodium ion removal from KCl solutions.

As shown in Figure 10(b), the KFeHCF electrode had a de-insertion peak at 0.47 V and an insertion peak at 0.2 V for the potassium ions. The peaks indicate that the potassium ions can be reversibly inserted into the structure of the KFeHCF electrode. Reportedly, the Prussian blue derivatives do not have a clear ionic selectivity (Trócoli et al., 2015), but have a higher thermodynamic preference for potassium ion intercalation than sodium ion (Erinmwingebovo et al., 2017). The galvanostatic charging/discharging test results in a KCl solution (refer to Figure 11(b)) showed a flat voltage profile in the 0.3 - 0.4 V range and it is also consistent with the CV results.

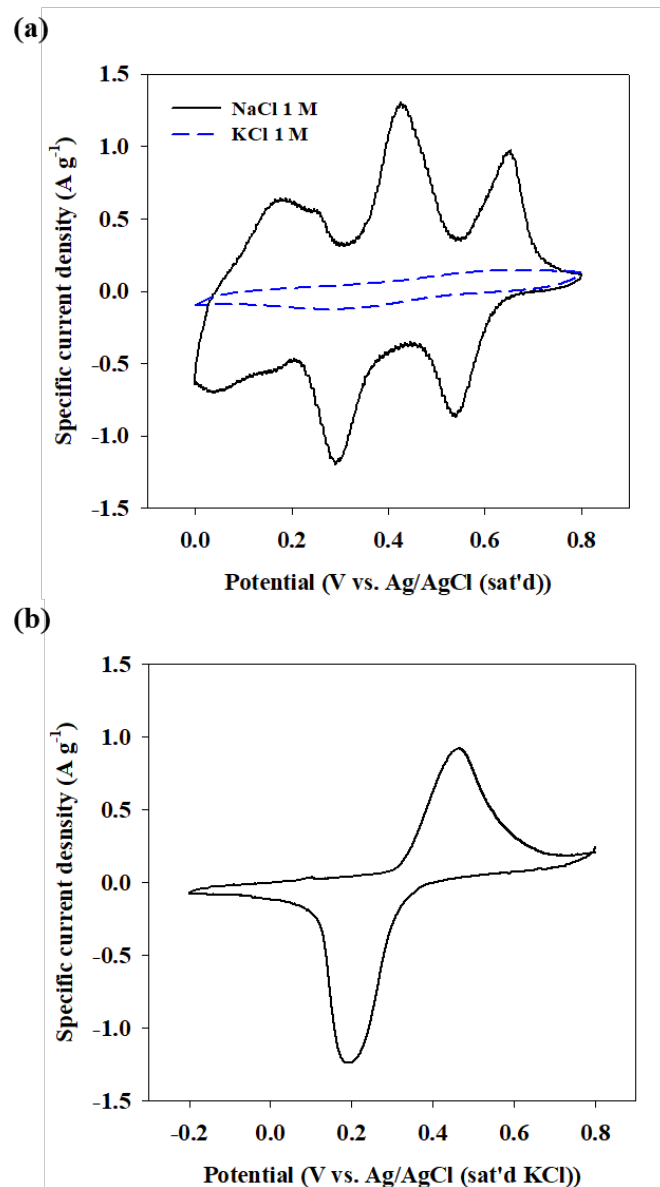


Figure 10. The cyclic voltammograms of (a) NMO electrode (NaCl, 1 M; black solid line & KCl, 1 M; blue dotted line) and (b) KFeHCF electrode (KCl, 1 M) (scan rate: 1 mV/s)

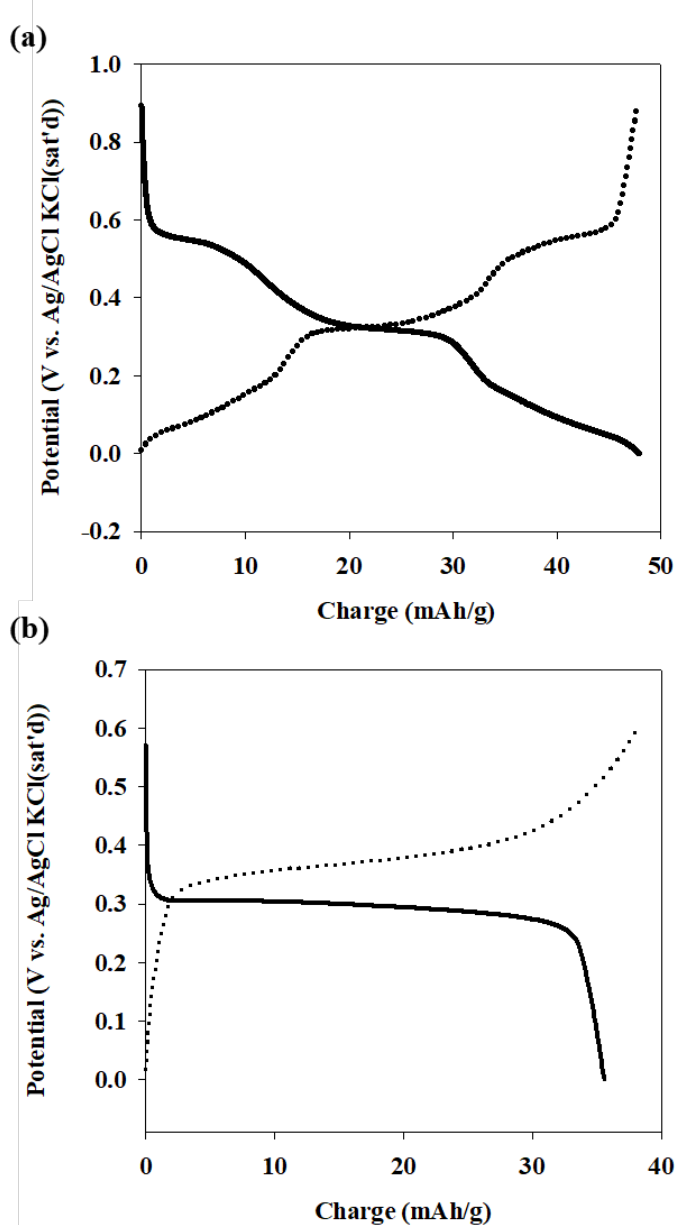


Figure 11. Galvanostatic charging and discharging voltage profile of **(a)** NMO electrode (NaCl 1 M; current density: 0.01 A/g) and **(b)** KFeHCF electrode (KCl 1 M; current density: 0.1 A/g)

4.2 Sodium removal with NMO/KFeHCF system

Figure 12 shows the changes in the sodium and potassium ion concentration ratios in the target KCl solution after the sodium ion removal step (Figure 12(a)) and in the reservoir KCl solution after the electrode regeneration step (Figure 12(b)), respectively, when the NMO/KFeHCF system was operated for 1 cycle. In the sodium ion removal step (1st step), the NMO electrode captures the sodium ions from the target solution, and the KFeHCF electrode releases the potassium ion that are already present in the electrode simultaneously (Figure 9). Following this operation principle, Figure 12(a) shows that approximately $18.7 \pm 2.6\%$ of the initial sodium ions in the target KCl solution (mixed solution of 20 mM NaCl and 40 mM KCl) were inserted into the NMO electrode. This is equivalent to 4.99 ± 0.70 mg of Na^+/g of NMO electrode] as calculated based on the mass of NMO. The coulombic efficiency calculated based on the amount of sodium ion removal was $76.2 \pm 10.7\%$. The standard deviation of 10.7% in the coulombic efficiency was not non-significant and this is partially related to the selectivity of NMO toward sodium ion. Referring to the previous study, the NMO showed approximately 13 times higher selectivity for Na^+ over K^+ (the ratio of $\text{Na}^+:\text{K}^+$ in the electrolyte was 1:1) (Kim et al., 2017). As the portion of K^+ became larger, the interference of K^+ is expected to be intensified in the intercalation of Na^+ into NMO, leading to the larger standard deviation (approximately 10% in this study). The potassium ions were released from the KFeHCF electrode as an accompanying reaction of the sodium ion removal by

the NMO electrode. As a result, the concentration of potassium ion was increased by $11.7 \pm 2.1\%$ compared with the initial concentration (40 mM).

In the electrode regeneration step (3rd step) shown in the diagram of Figure 9, the NMO electrode releases the sodium ions captured in the 1st step to the reservoir solution, while the KFeHCF electrode captures and replenishes the potassium ions from the electrolyte. As shown in Figure 12(b), the concentration of the sodium ions was increased and the concentration of the potassium ions was decreased by the 3rd step in the KCl reservoir solution. The sodium ions captured in the 1st step are thought to have been removed from the electrode; at the same time, the potassium ions were intercalated in the KFeHCF electrode, resulting in the compensation of the amount consumed in the 1st step. It indicates that the electrode regeneration step has progressed well without a significant loss of the coulombic efficiency. Therefore, it was confirmed that the NMO/KFeHCF system can be operated by rationally inserting and deinserting the sodium and potassium ions.

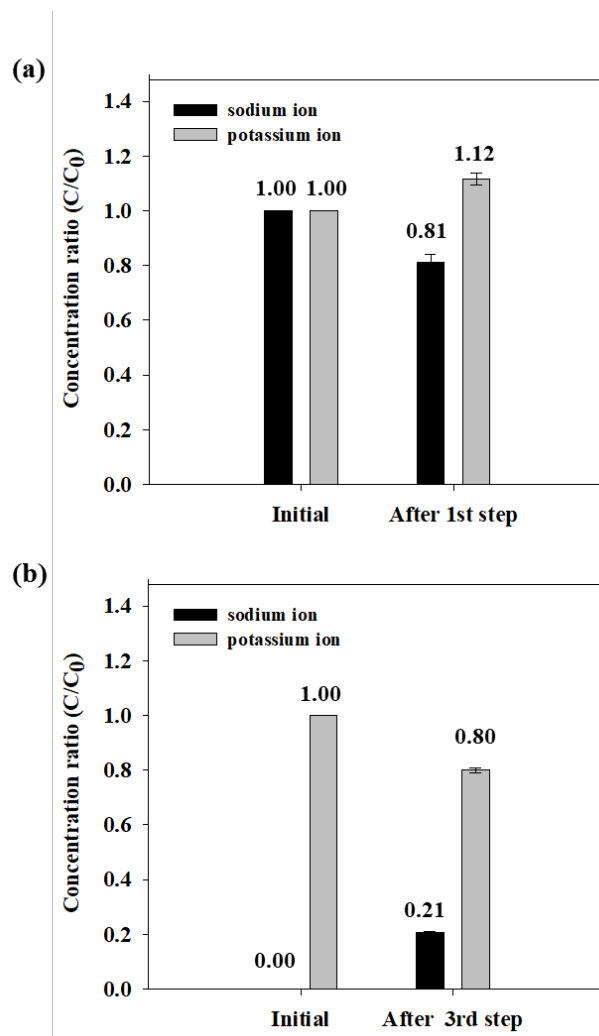


Figure 12. The concentration ratio of the sodium and potassium ions after (a) the sodium ion removal step (1st step) in the target KCl solution ($C_{0, K+} = 40 \text{ mM}$; $C_{0, Na+} = 20 \text{ mM}$) (current density: 0.3 mA/cm^2 , 1 h) and (b) the electrode regeneration step (3rd step) in the reservoir KCl solution ($C_{0, K+ \text{ or } Na+} = 20 \text{ mM}$, actual sodium ions are not present in the reservoir solution, but the C_0 of Na^+ was set to 20 mM to represent the concentration ratio)

4.3 Industrial application of NMO/KFeHCF system

To further demonstrate feasibility for the industrial applications, the NMO/KFeHCF system was operated in the industrial KCl solution (~ 4 M KCl) used as a raw material in the KCl electrolysis process in the actual KOH production industry. Figure 13(a) shows the concentration changes of the sodium ions when the electrochemical sodium ion removal process is run for several cycles. Note that 1 cycle means a continuous process from the 1st to the 4th step shown in Figure 9. After 3 cycles of operation, 36% of the initial sodium ion impurities were removed. The initial sodium ion removal rates of the 1st, 2nd, and 3rd were 13.3%, 13.0%, and 14.9%, respectively, without any significant decrease in system performance. This results suggest the possibility of continuous operation for the sodium ion removal process, which indicates that the product purity can be further increased by increasing the impurity removal rate when operating more cycles. The removal of sodium ion in the 1st cycle was about 13% (3.59 mg of Na⁺/[g of NMO electrode]) which is due to the reduction in coulombic efficiency as compared to the results obtained in the 40 mM KCl solution. The coulombic efficiency in 1st cycle operation was 54.3% and this result was attributed to higher interference of potassium ion in the electrolyte of approximately 4 M KCl. Despite of the relatively low coulombic efficiency, the electrochemical sodium ion impurity removal system was successfully investigated since the separation of sodium ion from the solution with high potassium ion concentration is a primary objective.

The voltage profile during the NMO/KFeHCF system operation is shown in Figure 13(b). As the 1st step (sodium ion removal step) progressed, the cell voltage decreased from about 0.35 V to -0.3 V on average for 3 cycles. This is because the voltage drops while the NMO electrode intercalates the sodium ions, and the voltage increases as the KFeHCF electrode releases the potassium ions. In the 3rd step (electrode regeneration step), the cell voltage increased from about 0 V to 0.8 V on average, because the opposite phenomenon was observed at both electrodes in the 1st step. The voltage profiles of 1st & 3rd step are slightly varying for each cycle because the concentration of sodium and potassium in the electrolyte and the state of the electrodes changed during the continuous cycle experiment.

The amount of energy consumed in one cycle of operation of this system can be calculated from the graph of the width of the voltage vs. charge shown in Fig. 4(b) as follows;

$$W = - \oint_C \Delta E dq$$

, where W is the energy(J); ΔE is the cell voltage(V), and q is the charge(C), respectively (La Mantia et al., 2011). An average of 5.53 J of energy was consumed per cycle during 3 cycles of operation in the industrial KCl solution (~ 4 M KCl). The energy consumption can be expressed as 4.46 Wh/(g of sodium ions) when converted to a unit of removing 1 g of sodium ions.

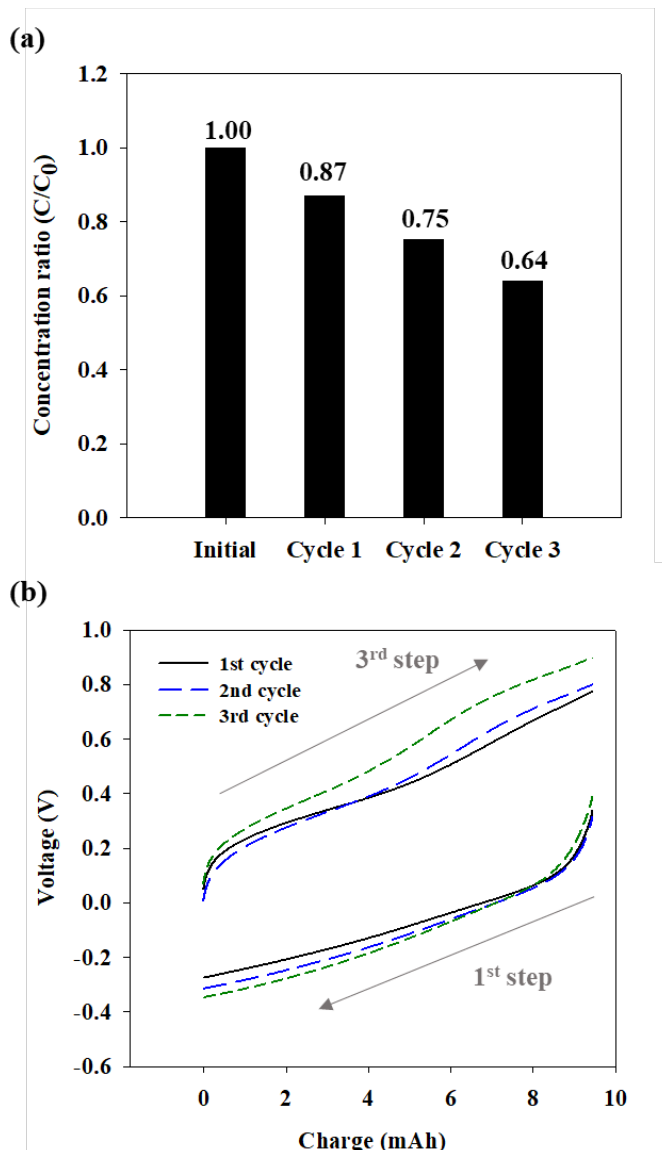


Figure 13. **(a)** The concentration ratio of sodium ions and **(b)** the voltage profile of the 1st step (sodium ion removal step) & 3rd step (electrode regeneration step) for 3 continuous cycles of operation in the industrial KCl solution (~ 4 M KCl solution with 20 mM NaCl as the impurity)

Chapter 5. Conclusion

In this study, it is demonstrated that the NMO/KFeHCF system successfully removed sodium ions selectively from a KCl solution. When the system was operated using actual industrial raw KCl materials, 36% of the initial sodium ions were removed after 3 cycles of operation, and the KCl purity increased to 99.8%. As investigated in this study, eco-friendly and energy-efficient electrochemical system technology can be applied to the purity control or the impurity removal. The electrochemical system using battery materials for impurity removal is expected to be developed and further applied to various materials in addition to KCl.

References

- Anderson, M.A., Cudero, A.L. and Palma, J., 2010. Capacitive deionization as an electrochemical means of saving energy and delivering clean water. Comparison to present desalination practices: Will it compete? *Electrochimica Acta*, 55(12): 3845-3856.
- Bergner, D., 1982. Membrane cells for chlor-alkali electrolysis. *Journal of Applied Electrochemistry*, 12(6): 631-644.
- Doeff, M.M., Peng, M.Y., Ma, Y. and De Jonghe, L., 1994. Orthorhombic Na x MnO₂ as a Cathode Material for Secondary Sodium and Lithium Polymer Batteries. *Journal of The Electrochemical Society*, 141(11): L145-L147.
- Erinmwingbovo, C., Palagonia, M.S., Brogioli, D. and La Mantia, F., 2017. Intercalation into a Prussian Blue Derivative from Solutions Containing Two Species of Cations. *ChemPhysChem*, 18(8): 917-925.
- Farmer, J.C., Fix, D.V., Mack, G.V., Pekala, R.W. and Poco, J.F., 1995. The use of capacitive deionization with carbon aerogel electrodes to remove inorganic contaminants from water, Low level waste conference, Orlando.
- Karyakin, A.A., 2001. Prussian blue and its analogues: electrochemistry and analytical applications. *Electroanalysis*, 13(10): 813-819.
- Kim, D.J. et al., 2013. Diffusion behavior of sodium ions in Na 0.44 MnO₂ in aqueous and non-aqueous electrolytes. *Journal of Power Sources*, 244: 758-763.
- Kim, S. et al., 2015. Lithium recovery from brine using a λ -MnO₂/activated carbon hybrid supercapacitor system. *Chemosphere*, 125: 50-56.
- Kim, S., Lee, J., Kim, C. and Yoon, J., 2016. Na₂FeP₂O₇ as a Novel Material for Hybrid Capacitive Deionization. *Electrochimica Acta*, 203: 265-271.
- Kim, S., Yoon, H., Shin, D., Lee, J. and Yoon, J., 2017. Electrochemical selective ion separation in capacitive deionization with sodium manganese oxide. *Journal of Colloid and Interface Science*, 506: 644-648.

- La Mantia, F., Pasta, M., Deshazer, H.D., Logan, B.E. and Cui, Y., 2011. Batteries for efficient energy extraction from a water salinity difference. *Nano letters*, 11(4): 1810-1813.
- Lee, H.-W. et al., 2014a. Manganese hexacyanomanganate open framework as a high-capacity positive electrode material for sodium-ion batteries. *Nature communications*, 5.
- Lee, J., Kim, S., Kim, C. and Yoon, J., 2014b. Hybrid capacitive deionization to enhance the desalination performance of capacitive techniques. *Energy & Environmental Science*, 7(11): 3683-3689.
- Lee, J., Kim, S. and Yoon, J., 2017. Rocking Chair Desalination Battery Based on Prussian Blue Electrodes. *ACS Omega*, 2(4): 1653-1659.
- Lee, J., Yu, S.-H., Kim, C., Sung, Y.-E. and Yoon, J., 2013. Highly selective lithium recovery from brine using a λ -MnO₂-Ag battery. *Physical Chemistry Chemical Physics*, 15(20): 7690-7695.
- Lu, Y., Wang, L., Cheng, J. and Goodenough, J.B., 2012. Prussian blue: a new framework of electrode materials for sodium batteries. *Chemical communications*, 48(52): 6544-6546.
- Osakabe, T., Imayoshi, S. and Hamamori, M., 2009. Method for Producing High Purity Caustic Potash. Google Patents.
- Paoletta, A. et al., 2017. A review on hexacyanoferrate-based materials for energy storage and smart windows: challenges and perspectives. *Journal of Materials Chemistry A*, 5(36): 18919-18932.
- Parant, J.-P., Olazcuaga, R., Devalette, M., Fouassier, C. and Hagenmuller, P., 1971. Sur quelques nouvelles phases de formule NaxMnO₂ ($x \leq 1$). *Journal of Solid State Chemistry*, 3(1): 1-11.
- Pasta, M., Battistel, A. and La Mantia, F., 2012a. Batteries for lithium recovery from brines. *Energy & Environmental Science*, 5(11): 9487-9491.
- Pasta, M., Wessells, C.D., Cui, Y. and La Mantia, F., 2012b. A desalination battery. *Nano letters*, 12(2): 839-843.

- Pasta, M., Wessells, C.D., Huggins, R.A. and Cui, Y., 2012c. A high-rate and long cycle life aqueous electrolyte battery for grid-scale energy storage. *Nature communications*, 3: 1149.
- Sauvage, F., Baudrin, E. and Tarascon, J.-M., 2007a. Study of the potentiometric response towards sodium ions of $\text{Na } 0.44 - x \text{ MnO}_2$ for the development of selective sodium ion sensors. *Sensors and Actuators B: Chemical*, 120(2): 638-644.
- Sauvage, F., Laffont, L., Tarascon, J.-M. and Baudrin, E., 2007b. Study of the insertion/deinsertion mechanism of sodium into $\text{Na}_0.44\text{MnO}_2$. *Inorganic chemistry*, 46(8): 3289-3294.
- Schultz, H., Bauer, G., Schachl, E., Hagedorn, F. and Schmittinger, P., 2000. Potassium Compounds, Ullmann's Encyclopedia of Industrial Chemistry. Wiley-VCH Verlag GmbH & Co. KGaA.
- Scrosati, B., 1992. Lithium rocking chair batteries: An old concept? *Journal of The Electrochemical Society*, 139(10): 2776-2781.
- Su, D., McDonagh, A., Qiao, S.Z. and Wang, G., 2017. High-Capacity Aqueous Potassium-Ion Batteries for Large-Scale Energy Storage. *Advanced Materials*, 29(1).
- Tani, Y. and Umezawa, Y., 1998. Alkali metal ion-selective electrodes based on relevant alkali metal ion doped manganese oxides. *Microchimica Acta*, 129(1): 81-90.
- Trócoli, R., Battistel, A. and La Mantia, F., 2015. Nickel Hexacyanoferrate as Suitable Alternative to Ag for Electrochemical Lithium Recovery. *ChemSusChem*, 8(15): 2514-2519.
- Trócoli, R., Erinmwingbovo, C. and La Mantia, F., 2016. Optimized Lithium Recovery from Brines by using an Electrochemical Ion-Pumping Process Based on $\lambda\text{-MnO}_2$ and Nickel Hexacyanoferrate. *ChemElectroChem*.
- Wang, R.Y. et al., 2015. Reversible multivalent (monovalent, divalent, trivalent) ion insertion in open framework materials. *Advanced Energy Materials*, 5(12).

- Wang, R.Y., Wessells, C.D., Huggins, R.A. and Cui, Y., 2013. Highly reversible open framework nanoscale electrodes for divalent ion batteries. *Nano letters*, 13(11): 5748-5752.
- Wessells, C.D., Peddada, S.V., Huggins, R.A. and Cui, Y., 2011. Nickel hexacyanoferrate nanoparticle electrodes for aqueous sodium and potassium ion batteries. *Nano letters*, 11(12): 5421-5425.
- Whitacre, J., Tevar, A. and Sharma, S., 2010. Na₄Mn₉O₁₈ as a positive electrode material for an aqueous electrolyte sodium-ion energy storage device. *Electrochemistry Communications*, 12(3): 463-466.
- Wu, X., Cao, Y., Ai, X., Qian, J. and Yang, H., 2013. A low-cost and environmentally benign aqueous rechargeable sodium-ion battery based on NaTi₂(PO₄)₃-Na₂NiFe(CN)₆ intercalation chemistry. *Electrochemistry communications*, 31: 145-148.
- Wu, X. et al., 2015. Vacancy-Free Prussian Blue Nanocrystals with High Capacity and Superior Cyclability for Aqueous Sodium-Ion Batteries. *ChemNanoMat*, 1(3): 188-193.

국문초록

수산화칼륨(KOH)은 포타슘을 함유한 화합물, 의약품, 비료 제조 및 반도체 공정 등 다양한 산업 분야에서 널리 쓰이고 있다. 전자재료 분야에서 사용되는 KOH는 99% 이상의 높은 순도를 요구하기 때문에 고순도 KOH의 경제적 가치는 매우 큰 편이다. 현재 KOH는 염화칼륨(KCl)의 전기분해를 통해 대량생산되고 있으며, 그렇기 때문에 생산되는 KOH의 순도는 원료인 KCl의 순도에 직접적으로 영향을 받는다. 보통 산업적으로 사용되는 KCl 원료의 경우, 소듐 이온 불순물을 함유하고 있기 때문에 결정화법을 통해 불순물을 제거한다. 하지만 소듐 이온 불순물의 농도가 높을 시에는 전처리 공정이 필요하다는 문제가 있다.

본 연구에서는 소듐 이온을 선택적으로 제거할 수 있는 전기화학적 배터리 시스템을 제안하고, 실제 KCl에 존재하는 불순물을 제거할 수 있는지 증명하였다. 전극 물질로는 수계 소듐 이온 배터리에 활용되고 있는 소듐 망간옥사이드($\text{Na}_{0.44}\text{MnO}_2$)와 프루시안 블루 물질 (KFeHCF)을 사용하였다. 본 연구의 주요 결과로 $\text{Na}_{0.44}\text{MnO}_2/\text{KFeHCF}$ 전극 배터리 시스템은 세 사이클 운전 후, 고농도의 KCl 용액 속에 들어있는 소듐 이온 불순물을 초기 대비 약 36% 정도 선택적으로 제거하였다. 이를

통해 KCl 의 순도를 99.8% 이상으로 증가시킬 수 있었으며, 따라서 경제적 가치가 높은 고순도 KOH 를 생산할 수 있는 가능성을 확인하였다. 전기화학적 배터리 시스템을 적용한 순도 제어 시스템은 KCl 뿐만 아니라 다양한 물질에 적용될 수 있을 것으로 기대되며, 또한 이와 같이 소듐 이온 배터리 전극 물질을 활용한 다양한 연구를 통해 탈염 기술 등을 더 발전시킬 수 있을 것으로 생각된다.

주요어: 전기화학적 시스템, 불순물 제거, 선택적 이온 분리, 소듐, 포타슘

학번: 2016-20995